

# G204D, a Mutation That Blocks the Proton-Conducting D-Channel of the *aa*<sub>3</sub>-Type Cytochrome *c* Oxidase from *Rhodobacter sphaeroides*<sup>†</sup>

Dan Han, Joel E. Morgan,<sup>‡</sup> and Robert B. Gennis\*

Department of Biochemistry and Chemistry, University of Illinois at Urbana–Champaign, 600 South Mathews Avenue, Urbana, Illinois 61801

Received June 14, 2005; Revised Manuscript Received July 15, 2005

**ABSTRACT:** Cytochrome *c* oxidase uses the free energy of oxygen reduction to establish a transmembrane proton gradient. The proton-conducting D-channel in this enzyme is the major input pathway for protons which go to the binuclear center for water formation (“chemical protons”) and likely the only input pathway for protons that get translocated across the lipid membrane (“pumped protons”). The D-channel starts at an acidic residue near the protein surface (D132, *Rhodobacter sphaeroides* numbering) and leads to another acidic residue near the binuclear center. Recent studies have shown that mutants that introduce an additional acidic residue in the channel (N139D) have the remarkable effect of accelerating steady-state oxidase activity but completely eliminating proton pumping. In this work, an aspartic acid was introduced at the position of glycine 204, G204D, which is also within the D-channel, and the effects were examined. In contrast to N139D, the G204D mutation results in a dramatic decrease of the steady-state oxygen reductase activity (<2% of wild type) [Aagaard, A., and Brzezinski, P. (2001) *FEBS Lett.* 494, 157–160]. The residual activity is not coupled to the proton pump, and furthermore, in reconstituted vesicles the mutant enzyme exhibits a reverse respiration control ratio; i.e., the mutant oxidase activity is stimulated rather than inhibited when working against a protonmotive force. Hence, the mutant behaves very much like the D132N, which blocks proton uptake through the D-channel. Single-turnover experiments show that the rate-limiting step in the reaction of O<sub>2</sub> with the fully reduced G204D mutant is the F → O transition, similar to the D132N mutant. The block of the D-channel in the D132N mutant can be partly bypassed by biochemically removing subunit III from the enzyme, indicating that removal of the subunit reveals an alternate entrance for protons to the channel. However, this is not observed with the G204D mutant. This suggests that the cryptic entrance to the D-channel that is revealed by the removal of subunit III is between the levels of G204 and D132.

Cytochrome *c* oxidase is an integral membrane metallo-protein that couples the four-electron reduction of dioxygen to water to the translocation of protons across a lipid bilayer (2, 3). The proton gradient created by this catalysis is used in various energy-requiring processes, including the synthesis of ATP. Extensive studies have been done to elucidate the mechanisms by which the enzyme translocates protons and couples this with the chemical reaction (3–5).

On the basis of the crystal structures (6) and mutagenetic studies (7, 8), two proton transfer pathways have been suggested for the prokaryotic oxidases: the K-channel and the D-channel (Figure 1). The K-channel has an entrance at E101 in subunit II (9) and extends to Y288, located at the enzyme active site. The K-channel contains a critical lysine residue (K362) in the middle. Studies on the K-channel mutations suggest that the K-channel is required for the transfer of at least one and, possibly, two protons to the binuclear center upon reduction of heme *a*<sub>3</sub> and Cu<sub>B</sub> (10–

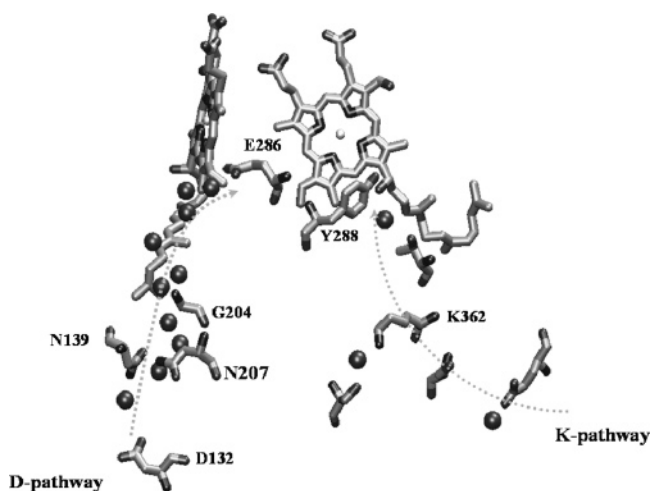


**FIGURE 1:** Selected residues that define the proton-conducting channels of the *R. sphaeroides* oxidase in relation to heme *a* (left) and heme *a*<sub>3</sub> (right). The spheres are water molecules observed in the X-ray structure of the oxidase (29). The Cα–Cα distances are 13.96 Å for D132–G204, 14.86 Å for G204–E286, and 26.74 Å for D132–E286. The software used for this figure was VMD (32).

<sup>†</sup> This research was supported by a grant from the National Institutes of Health (HL16102 to R.B.G.).

\* To whom correspondence should be addressed: phone, (217) 333-9075; fax, (217) 244-3186; e-mail, r-gennis@uiuc.edu.

<sup>‡</sup> Current address: Department of Biology, Jonsson-Rowland Science Center, Rensselaer Polytechnic Institute, 110 8th St., Troy, NY 12180.

12). No data implicate the K-channel in a direct role in proton pumping, though this possibility cannot be excluded.

The D-channel appears to be responsible for the input of all other protons from the N (negative) side of the membrane, including the four protons (per O<sub>2</sub>) that are pumped across the membrane. The D-channel extends from an aspartic acid (D132) at the entrance of the channel to a glutamic acid (E286) about 25 Å away from D132 and 12 Å away from the binuclear center. A chain of about 10 water molecules defines the channel pathway and presumably provides a hydrogen bond network to facilitate proton transfer from D132 to E286 (Figure 1). It appears that E286 is a branch point and that some protons are transferred from E286 to the binuclear center to form water, whereas other protons are transferred to an exit pathway to be pumped out.

Replacement of D132 by either asparagine (D132N) or alanine (D132A) results in an enzyme with <5% turnover and eliminates proton pumping (7, 13). The E286Q mutation in the *Rhodobacter sphaeroides* oxidase virtually eliminates turnover (<0.5%) (14). Recently, another mutation in the D-channel, N139D, was shown to completely decouple the oxidase activity from the proton pump (15, 16). The mutant enzyme has twice the specific oxidase activity as does the wild-type oxidase, but the mutant does not pump protons. The placement of the acidic residue in the N139D mutant increases the apparent pK<sub>a</sub> of residue E286, and it is speculated that this may inhibit proton transfer from E286 to the putative accepting group in the exit channel (17, 18).

The current work was motivated to determine the effect of placing an acidic residue at a different location in the D-channel. As shown in Figure 1, G204 is located just "above" N139 within the D-channel. Modeling suggested that replacing the glycine by an aspartate should position the carboxyl group of the aspartate within the D-channel. Previously, the equivalent residue in the *Paracoccus denitrificans* oxidase was replaced by phenylalanine and tryptophan, and in both cases, the mutations only caused moderate reduction in turnover and no influence on proton pumping (16).

The G204D mutant was made in the *R. sphaeroides* oxidase, and the enzyme was purified and examined. The G204D mutant does not behave like the decoupling N139D mutant but is much more similar to the D132N mutant. The G204D mutation appears to block proton transfer through the D-channel to E286. This is the first example of a mutation in the middle of the D-channel which effectively prevents proton transfer through the channel.

The property of blocking proton transfer was utilized to help to localize the cryptic entrance to the D-channel that is created by the removal of subunit III. This new proton entry partially reverses the block caused by the D132N mutation. However, removing subunit III does not result in bypassing the block due to the G204D mutation. Hence, the new entry that is uncovered by removal of subunit III must lie between G204 and D132, perhaps H26, as previously speculated (19).

## MATERIALS AND METHODS

**Site-Directed Mutagenesis.** The G204D mutant was constructed using the Quikchange site-directed mutagenesis kit from Stratagene. Primers were synthesized at the University of Illinois Biotechnology Center, Urbana. The gene was partially sequenced to verify the mutation.

**Protein Purification.** His-tagged wild-type and mutant enzymes were purified from *R. sphaeroides* using histidine

affinity chromatography as described previously (20). Further purification of the enzyme is needed for proton-pumping measurement (21). About 4 mg of purified enzyme was diluted into about 1 mL of buffer A (10 mM KH<sub>2</sub>PO<sub>4</sub>, 1 mM EDTA, 0.1% DM,<sup>1</sup> pH 7.2) and loaded onto a tandem DEAE-5PW column (Toso-Haas) attached to an FPLC system (Amersham-Pharmacia Biotech ÄKTA Basic). The columns were washed with buffer A, and the enzyme was eluted at a flow rate of 0.5 mL/min with a gradient of buffer B (buffer A with 1 M KCl). The gradient was designed to go to 15% buffer B within 0.5 column volume, and then the oxidase was eluted as the gradient was slowly increased from 15% to 45% buffer B over 4 column volumes. Two peaks were resolved, and the second peak was collected for proton pumping assay.

**Steady-State Activity.** Steady-state oxidase activity was measured polarographically using a YSI model 53 oxygen meter equipped with a water-jacketed and stirred glass measuring vessel. The reaction mixture contains 1.8 mL of 50 mM potassium phosphate buffer, 0.1% DM, pH 6.5, 10 mM ascorbate, 0.5 mM TMPD, and 30 μM horse heart cytochrome *c*. For experiments with reconstituted cytochrome oxidase vesicles, the buffer used was 100 mM HEPES–KOH and 0.1% DM, pH 7.4. The enzyme turnover (mole of electrons per second per mole of enzyme) was calculated from the slope of the oxygen consumption traces and corrected for background in the absence of the enzyme.

**Reconstitution of Oxidase into Vesicles.** Cytochrome oxidase vesicles (COVs) were made by using Bio-Beads to remove detergent, as described (22, 23). Asolectin (80 mg/mL) was mixed with 2% cholic acid and 100 mM HEPES–KOH, pH 7.4, and then sonicated using a model W-375 sonicator (Heat System-Ultrasonics, Inc., now Mixonix, Inc., Farmingdale, NY) using 10–12 30 s cycles, at 50% duty, with a break of ~60 s between cycles. The mixture was kept on ice under a stream of argon gas during sonication. The oxidase was added to the lipid/cholate mixture to yield a concentration of ~1.2 μM (the same protein-to-lipid ratio was used for both wild-type and mutant enzyme). The mixture was stirred at 4 °C with 66 mg of Bio-Beads/mL added every 30 min. After 4 h, 100 mM HEPES–KOH buffer was added (0.5 mL/mL of mix), and the mixture was brought to room temperature. Bio-Beads were added every 30 min for another 3 h (133 mg/mL during the first 2 h and 266 mg/mL during the last hour). The proteoliposomes were pipetted so as to remove the Bio-Beads and then dialyzed overnight against 60 mM KCl.

**Proton Pumping Measurement.** Proton pumping was measured by monitoring the pH changes outside the COVs during enzyme turnover. A 1.5 mL reaction mixture containing 60 mM KCl, 40 μM cytochrome *c*, 300 μM ascorbate, 10 μM valinomycin, and ~0.4 μM oxidase was placed in an anaerobic stirred cell with a sensitive glass pH electrode. After all of the components were added except the reductant (and perhaps valinomycin), the headspace of the cell was flushed with a constant stream of water-saturated argon.

<sup>1</sup> Abbreviations: CCCP, carbonyl cyanide *p*-(trifluoromethoxy)-phenylhydrazone; TMPD, *N,N,N',N'*-tetramethyl-*p*-phenylenediamine; DM, *n*-dodecyl β-D-maltoside; Ni-NTA, nickel nitrilotriacetic acid; HEPES, 4-(2-hydroxyethyl)piperazine-1-ethanesulfonic acid; RCR, respiratory control ratio.

Stirring under this argon atmosphere for some minutes removed the O<sub>2</sub> from the sample. The reductant was then added. The pH electrode was attached to a sensitive pH meter and a digitizer. The reaction was initiated by adding air-saturated H<sub>2</sub>O equilibrated at 25 °C to the reaction mixture (256 μM O<sub>2</sub>). Calibration was done by addition of the same volume of a solution of 1 mM HCl. The experiment was repeated in the presence of 30 μM protonophore CCCP to equilibrate the protons on the inside and outside of the vesicles.

**Reduction Kinetics.** Reduction kinetics was studied using an Applied Photophysics stopped-flow spectrophotometer equipped with a diode array detector as described (24, 25). The solution containing the oxidase (5 μM enzyme in 50 mM Tricine, pH 8.0, and 0.1% DM) was loaded in one of the driving syringes of the stopped-flow device. Buffer containing 10 mM ruthenium(III) hexamine was mixed with 30 mM dithionite, and the mixture was loaded into the other driving syringe. Upon mixing, the oxygen in the solution is quickly removed by reaction with dithionite, and the enzyme is subsequently reduced by the ruthenium and dithionite mixture.

**Oxidation Kinetics.** Oxidation kinetics was studied with the same equipment as described in the study of reduction kinetics. A solution containing the enzyme (4 μM oxidase and ~100 μg/mL catalase in 50 mM Tricine, pH 8.0, and 0.1% DM) was placed in a reservoir made from a syringe barrel at the loading position of the stopped-flow unit. The solution was made oxygen free by directing a gentle jet of water-saturated argon gas onto the surface of the sample. About 400 μM dithionite was added to reduce the enzyme, and then the sample was loaded into one of the driving syringes. The presence of catalase eliminates any hydrogen peroxide that might be generated by the dithionite and, thus, prevents formation of P and F intermediates of the oxidase. Oxygen-saturated Tricine buffer was loaded into the other driving syringe. Upon mixing, the dithionite is rapidly eliminated by reaction with excess O<sub>2</sub>, and the reduced enzyme is subsequently oxidized by O<sub>2</sub>.

**Subunit III Depletion.** Subunit III was removed from the oxidase which had been affinity purified using the Ni-NTA column as described in ref 19.

## RESULTS

**Steady-State Activity.** Both the wild-type and the G204D mutant enzymes were purified using a Ni-NTA affinity column. The UV-vis spectra of the mutant enzyme showed no difference from the wild-type spectra (data not shown), indicating that, in the G204D mutant enzyme, the hemes are intact and the mutation does not result in any major structural perturbation. The turnover number of the G204D enzyme is ~23 e<sup>-</sup>/s, compared to ~1200 e<sup>-</sup>/s for the wild-type enzyme (Table 1). Hence, the G204D mutation reduces the specific activity to only ~2% of the activity of the wild-type control.

**Respiration Control Ratio (RCR).** The G204D mutant and the wild-type enzymes were each reconstituted into phospholipid vesicles using the Bio-Beads method (22, 23). The activities of the wild-type and the mutant enzymes after reconstitution were assayed in the presence and in the absence of the ionophores valinomycin and CCCP (Table 1). In the absence of the ionophores, oxidase turnover results

Table 1: Comparison of Wild-Type and Mutant Oxidases: Activity before and after Reconstitution, Respiratory Control Ratio, and Proton Pumping Efficiency

|           | activity [e <sup>-</sup> /(s·aa <sub>3</sub> )] |                       |      |            |                  |                                |
|-----------|---|-----------------------|------|------------|------------------|--------------------------------|
|           | solubilized protein <sup>a</sup>                | vesicles <sup>b</sup> |      |            | RCR <sup>c</sup> | H <sup>+</sup> /e <sup>-</sup> |
|           |   | initial               | +Val | +Val, CCCP |                  |                                |
| wild type | 1280 ± 79.0                                     | 110                   | 160  | 480        | ~4               | 0.5–0.6                        |
| G204D     | 23 ± 1.6  | 12                    | 8    | 13         | ~1               | 0                              |

<sup>a</sup> The activity of the solubilized enzyme was measured as described in Materials and Methods. The reaction was initiated by adding about 3 nM wild-type enzyme or 0.3 μM G204D mutant enzyme. The rates of nonenzymatic reduction of O<sub>2</sub> by ascorbate/TMPD were subtracted. The values are the average of measurements on five different preparations of enzyme. <sup>b</sup> It was assumed for the purposes of quantitation that all of the enzyme added to the reconstitution mixture was reconstituted into vesicles in the correct orientation. <sup>c</sup> The respiratory control ratio (RCR) was calculated by dividing the activity measured in the presence of both valinomycin and CCCP by the initial activity, measured in the absence of the ionophores.

in a proton electrochemical gradient (protonmotive force) which inhibits the oxidase activity. Addition of the protonophore (CCCP) and ionophore (valinomycin, in the presence of K<sup>+</sup>) eliminates the protonmotive force, and with the wild-type oxidase, the result is to accelerate the steady-state oxidase activity since the transmembrane charge movement inherent in the enzyme mechanism is no longer working against the electrochemical gradient. This is measured by the RCR, which is the ratio of enzyme activity in the presence of the ionophores divided by the activity in the absence of the ionophores. The expected result was found for the wild-type oxidase, which had an RCR of 4 (Table 1 and Figure 2). This response also indicates that the vesicles are intact and do not exhibit excessive proton leakage. In contrast, the G204D mutant has about the same activity in the presence of both valinomycin and CCCP, but the activity is decreased in the presence of valinomycin alone [8 vs 12 e<sup>-</sup>/(s·aa<sub>3</sub>)] (Table 1 and Figure 2), resulting in an RCR close to 1. The fact that the reconstituted G204D mutant did respond to the change of protonmotive force across the membrane in the presence of valinomycin indicates that the vesicle membrane is intact. The fact that the activity is decreased in the presence of valinomycin rather than increased is reminiscent of results obtained with the D132N and D132A mutants in reconstituted vesicles which have a more pronounced reverse RCR (7, 13).

**Proton Pumping.** Using a pH meter, the proton pumping of the oxidase was measured using the enzyme reconstituted in phospholipid vesicles. The reaction is initiated by the addition of a known amount of O<sub>2</sub> present in water, sufficient for the enzyme to turn over about 20–40 times. Figure 3 shows that, with the wild-type enzyme, there is a rapid acidification followed by slow alkalinization of the solution due to slow proton leakage back into the vesicles. The proton pumping (H<sup>+</sup>/e<sup>-</sup>) is in a range normally observed with the *R. sphaeroides* oxidase (0.5–0.8, with 1.0 being the expected value). In contrast, the G204D mutant oxidase (Figure 3B) exhibits no acidification, only alkalinization, indicating that there is no proton pumping associated with the turnover of this enzyme. Note that, with both the wild-type and mutant oxidases, the addition of CCCP allows rapid proton equilibration across the membrane and, as a result, only net rapid

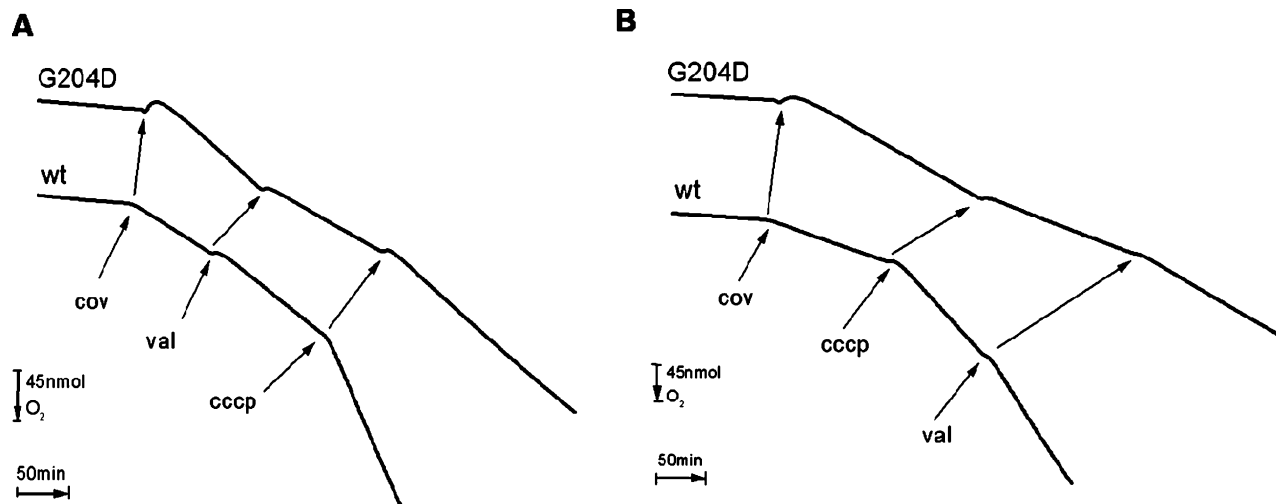


FIGURE 2: Comparison of the effects of valinomycin and CCCP on the oxygen consumption of reconstituted wild-type and G204D oxidases. Oxygen consumption was monitored polarographically, and the conditions were the same as for reconstituted oxidases described in Table 1. The effects are shown for (A) the addition of valinomycin ( $14 \mu\text{M}$ ) followed by CCCP ( $28 \mu\text{M}$ ) or (B) the addition of CCCP followed by valinomycin. In this experiment, the G204D enzyme is 12 times more concentrated than wild-type oxidase.

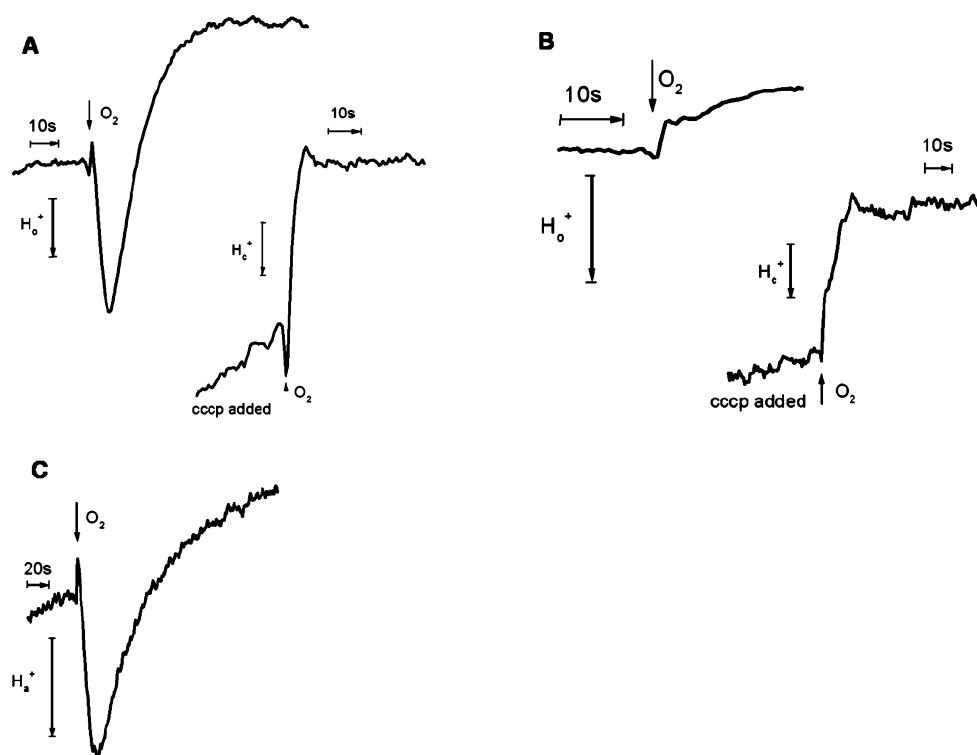


FIGURE 3: Proton pumping by the wild-type (A) and G204D mutant oxidase (B, C). The assay was performed with a stirred anaerobic cell equipped with a sensitive pH meter. The reaction mixture includes 60 mM KCl, 40  $\mu\text{M}$  cyt *c*, 300  $\mu\text{M}$  ascorbate, 10  $\mu\text{M}$  valinomycin, and wild-type or G204D enzyme in reconstituted vesicles. The protein:lipid ratio in the vesicles is identical for the two samples, but more vesicles were added to the reaction mixture of G204D oxidase to obtain a comparable activity to that of the wild-type sample. The reaction was initiated by adding 2.5 nmol of  $\text{O}_2$  (10  $\mu\text{L}$  of  $\text{H}_2\text{O}$ ) into the reaction mixture. pH changes in the bulk solution (outside the vesicles) were measured. Rapid acidification occurred upon addition of  $\text{O}_2$  to the wild-type oxidase (A) but not in the case of the G204D mutant (B). In the presence of CCCP, addition of  $\text{O}_2$  produced the expected alkalinization in both cases. (C) shows the pH change outside G204D vesicles when the ascorbate concentration is increased to 7 mM.

consumption of protons is observed. This shows that the G204D reconstituted vesicles are intact. Figure 3C shows the pH response of the G204D vesicles with a high concentration of ascorbate (7 mM). The rapid acidification is due to the rapid proton release from the reaction between ascorbate and cytochrome *c*, which confirms that the mutant enzyme is inserted properly in the vesicles.

**Oxidation and Reduction Kinetics.** To further investigate which part of the reaction cycle is slowed by the G204D

mutation, oxidation and reduction kinetics were performed using a stopped-flow spectrophotometer. To study the oxidation kinetics, the fully reduced enzyme was rapidly mixed with oxygen-saturated buffer. Figure 4A shows the absorption changes at 445 nm for both the wild-type and G204D mutant enzyme during this process. A majority of the reaction with the wild-type enzyme was complete within the dead time of mixing. From the remaining part of the reaction, we can only know that the rate constant for the



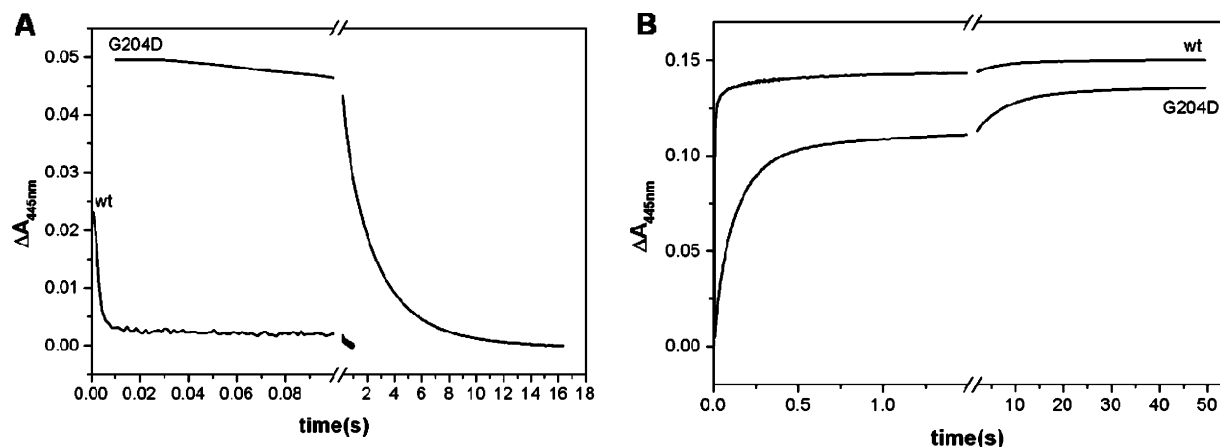


FIGURE 4: (A) The kinetics of oxidation by O<sub>2</sub> of the fully reduced enzymes and (B) the kinetics of reduction by ruthenium(II) hexamine of the fully oxidized enzymes. Measurements were made with both the wild-type and the G204D mutant oxidases. Absorption is normalized to the zero time point. The conditions are described in the text.

Table 2: Effect of Removing Subunit III on the Steady-State Activity of the Wild-Type and Mutant Oxidases

| oxidase   | activity [ $e^-/(s \cdot aa_3)$ ] at pH 7.5 |                 |
|-----------|---|-----------------|
|           | (+) subunit III                             | (-) subunit III |
| wild type | 1118  | 442             |
| D132N     | 24.3  | 101.1           |
| G204D     | 28.3  | 4.4             |

wild-type enzyme is higher than 480 s<sup>-1</sup>. In the mutant enzyme, the oxidation rate is dramatically decreased (more than 960-fold) with a rate constant of 0.5 s<sup>-1</sup>. When the data surfaces were analyzed using the global multiexponential fitting program SPLMOD (26), the spectra show that the F-to-O transition of the G204D mutant is the rate-limiting step during oxidation (data not shown).

The rate of reduction of the fully oxidized enzyme by ruthenium(III) hexamine was also determined by monitoring the absorption changes at 445 nm (Figure 4B). These data show that the rate of reduction of heme a<sub>3</sub> is slowed by the G204D mutation compared to the wild-type oxidase. Rate constants of 170 and 8 s<sup>-1</sup> were obtained for the wild-type and G204D mutant enzymes, respectively.

**Effects of Removal of Subunit III.** The removal of subunit III from the wild-type oxidase results in a lower steady-state activity (by about 60% at pH 7.5), apparently by impeding proton flux through the D-channel (19, 27, 28). This is also shown in Table 2 and Figure 5A. However, the removal of subunit III substantially increases the steady-state turnover of the D132A mutant at pH 7.5 (19). To determine the influence of subunit III depletion on the activity of the G204D mutant, subunit III was removed from the wild-type oxidase as well as from the D132N and G204D mutants (creating WT III<sup>-</sup>, D132N III<sup>-</sup>, and G204D III<sup>-</sup>) by treating with Triton X-100 as described previously (19). SDS-PAGE analysis confirmed that subunit III was completely removed (data not shown). The UV-vis spectra of the subunit III-depleted oxidases were unchanged, indicating that the removal of subunit III does not perturb the environments of the heme centers.

As shown in Table 2 and Figure 5B, the depletion of subunit III also increases the activity of the D132N mutant, similar to what is observed with the D132A mutant (19, 27). Since these mutations are thought to block the entrance of

protons into the D-channel, it has been concluded that an alternative proton entrance is revealed when subunit III is removed, thus bypassing the block at D132. In contrast, removal of subunit III almost completely eliminates the activity of the G204D mutant (Table 2 and Figure 5C). At the very least, the data indicate that the potential new entrance for protons that is recruited in the absence of subunit III is at a position below the level of G204 in the D-channel, which is not surprising since the region of the protein above G204 is presumably buried within the membrane bilayer. The removal of subunit III and the G204D mutation act as a double block of the D-channel.

**Effects of Adding Arachidonic Acid.** Previous work has shown that arachidonic acid can partially overcome the proton block due to the D132A and D132N mutations (13, 27). Presumably, the hydrophobic fatty acid binds in a manner to provide a pathway for protons to enter the channel. The same experiment was performed with the G204D mutant. The results (Table 3) show that arachidonic acid can also partially provide a bypass around the G204D block to approximately the same extent observed with the D132A and D132N mutants. Note that, even in the presence of arachidonic acid, the activity of the mutants is still far less than that of the wild-type oxidase. Nevertheless, the data suggest that the influence of arachidonic acid is not specifically at the D132 site, substituting for the missing carboxyl group in the D132N or D132A mutants. Instead, the effect of the fatty acid appears to permit proton leakage into the D-channel even for a block that is considerably higher up in the channel. The specific nature of the interaction of arachidonic acid with the oxidase is not known, and the question of how the fatty acid facilitates proton entry into the D-channel must remain for future studies (see Figure 1).

**Effect of Arachidonic Acid on the Subunit III-Depleted Oxidases.** The addition of arachidonic acid to the wild-type oxidase has no influence on the specific activity (Table 3). However, the presence of arachidonic acid increases the oxidase activity of the subunit III-depleted oxidase. This is shown in Figure 6A. At pH 7.5, the activity of the subunit III-depleted oxidase is about half of that of the intact enzyme, as previously shown (27). Addition of arachidonic acid at pH 7.5 brings the activity up to about that expected for the intact enzyme. Removal of subunit III also greatly enhances

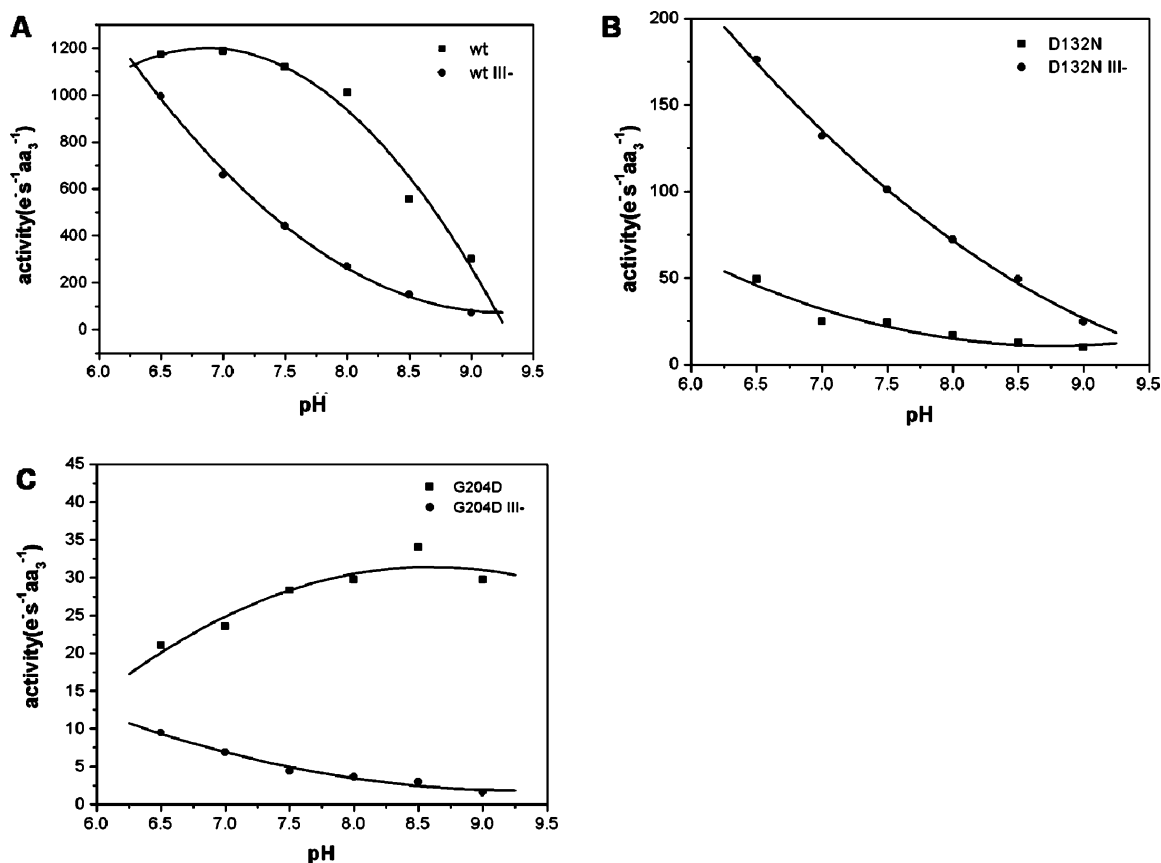


FIGURE 5: Effects of removal of subunit III on the pH dependence of the steady-state activity of the wild-type and mutant oxidases.

Table 3: Effect of Arachidonic Acid (AA) on Steady-State Activity of Wild-Type and Mutant Oxidase

| oxidase   | % activity <sup>a</sup> |                      |
|-----------|-------------------------|----------------------|
|           | 5 $\mu\text{M}$ AA      | 250 $\mu\text{M}$ AA |
| wild type | 100                     | 100                  |
| G204D     | 160                     | 260                  |
| D132N     | 130                     | 290                  |

<sup>a</sup> Oxygen consumption of the purified, soluble enzymes was measured at pH 6.5, as described in Materials and Methods. 100% represents the turnover of the corresponding enzyme before adding arachidonic acid.

the effect of arachidonic acid on the proton block caused by the D132N mutant. The activity of this mutant is greatly enhanced by adding arachidonic acid to the enzyme that has been depleted of subunit III (Figure 6B). It is shown in Figure 6C that the effect of adding arachidonic acid to the G204D mutant also is greatly enhanced by the removal of subunit III. These data suggest that the arachidonic acid effect is to enhance proton entry to the D-channel above the level of G204 and that removal of subunit III makes the enzyme much more susceptible to this effect.

## DISCUSSION

The substitution of glycine 204 by aspartate leads to a 98% reduction in turnover rate and complete elimination of proton pumping in the *R. sphaeroides*  $\text{aa}_3$ -type oxidase. The same residue in *P. denitrificans* oxidase has been mutated to phenylalanine and tryptophan, and only moderate reduction of turnover rate was observed, without any major effect on the stoichiometry of protons pumped in the reconstituted

enzyme (16). Clearly, a block to proton conduction has been introduced in the middle of the D-channel by the G204D mutation. In the X-ray structure, 10 water molecules have been identified in the D-channel, presumably forming a hydrogen-bonding network with other amino acids in the channel (29). Unlike the previously studied mutations D132N and D132A, in which the proton-collecting function of the D-channel is also interrupted, the introduced D204 might disturb the hydrogen-bonding network in the channel. Two water molecules in the D-channel are quite close to G204, with the distances of O—C $\alpha$  at 4.1 and 3.4 Å, respectively. When the glycine is substituted by aspartate, it is very likely that the carboxylate group of D204 will form hydrogen bonds with water molecules and disrupt the original hydrogen bonds that provide a proton-conducting pathway.

Analysis of the reaction of the reduced G204D mutant oxidase with  $\text{O}_2$  shows that the rate-limiting step during the turnover of the G204D enzyme is likely to be the F-to-O transition. This is similar to what has been observed with the block caused by the D132N mutant oxidase (30). In single turnover, the proton present on E286 is used in the  $\text{P}_R$ -to-F transition. Presumably, because of the disturbance of the hydrogen-bonding network in the D-channel by the G204D mutation, E286 cannot be reprotonated rapidly, resulting in a severely reduced rate of the F-to-O transition. From the data presented here and previously (16), it is not very likely that the substitution of G204 by an aspartate or amino acids with bulky side chains causes any structural changes in the protein which can lead to functional alteration.

One unexpected observation with the G204D mutant is that the rate of reduction of the binuclear center is slower ( $\sim 20$ -fold) than observed with the wild-type oxidase. This

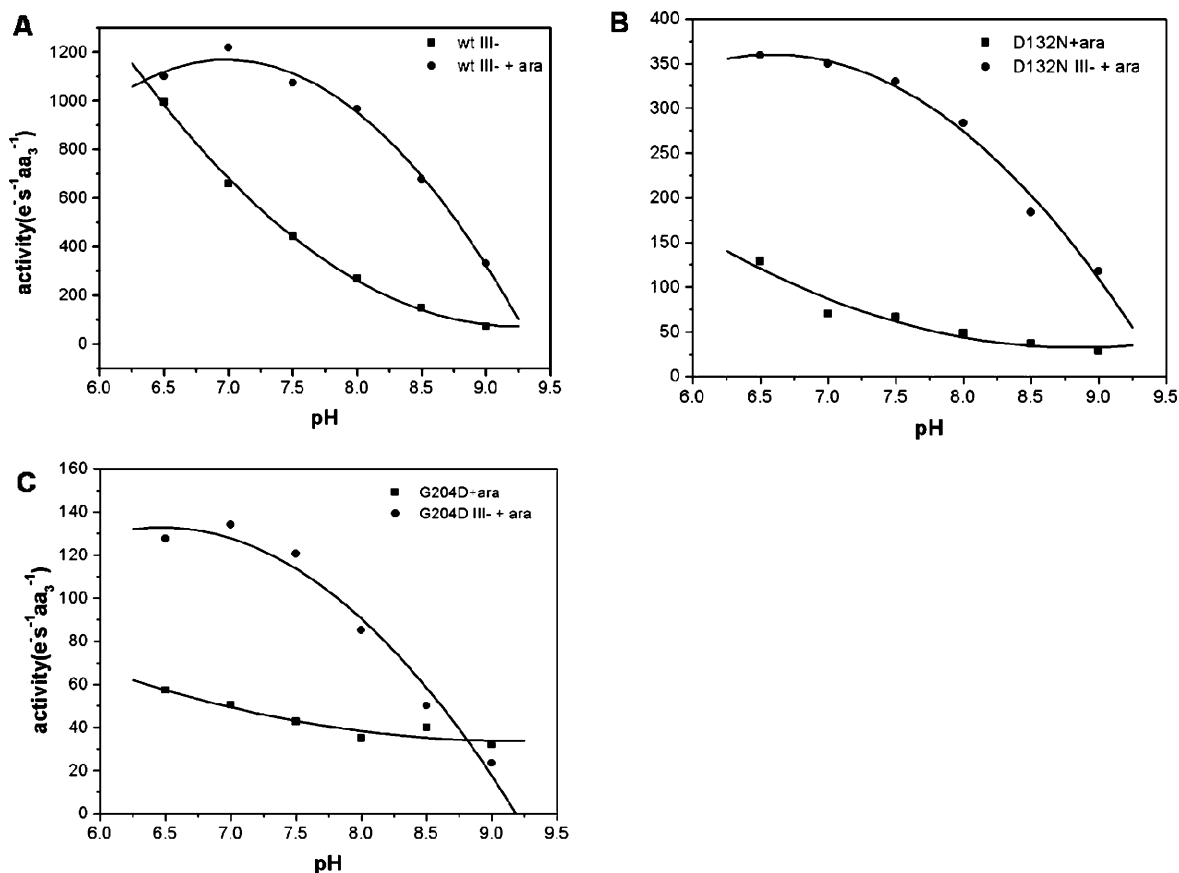


FIGURE 6: Effects of arachidonic acid (250  $\mu$ M) on the pH dependence of the steady-state activity of wild-type and mutant oxidases.

is not the pattern observed with D132N (10). This may indicate a role of the D-channel in proton uptake during the reductive phase, as has been suggested previously (10), but further work will be necessary before such a conclusion is justified.

It is clear, however, that proton uptake through the D-channel is effectively blocked by both the D132N (or D132A) and G204D mutant enzymes. It was previously shown that D132N and D132A both show an anomalous behavior insofar that the oxidase activity of the mutant enzymes in reconstituted vesicles is inhibited rather than being stimulated by the presence of either an ionophore (valinomycin) or the protonophore (CCCP) (7). This yields an RCR value that is less than 1. The same is true of the G204D mutant, at least in the presence of valinomycin. The pattern manifested by the G204D mutant is similar to that shown by the D132N mutant (7). This is that they exhibit a reverse respiration control ratio (RCR) when reconstituted into lipid vesicles. Their activities are inhibited rather than stimulated by release of either the proton or the electrical gradient. A model has been proposed (13) to explain this phenomenon, which basically involves protons leaking in through the exit channel to support a low level of enzyme turnover. This explanation could apply just as well for the G204D mutant as for the D132N mutant.

In the case of the D132N or D132A mutants, the addition of arachidonic acid stimulates the activity by severalfold and also eliminates the reverse respiratory control (13). In the current work, it is also demonstrated that the activity of the G204D mutant is similarly stimulated by arachidonic acid (Table 3). Presumably, the hydrophobic fatty acid binds in

such a way so as to slightly loosen the structure of the enzyme and allow protons to enter the D-channel. At least part of this effect must occur at a level above G204, i.e., between G204 and E286 (see Figure 1). The effect of arachidonic acid in the case of G204D, D132N (Figure 6), and also D132A (19) is greatly enhanced by removing subunit III by treating the enzyme with excess Triton X-100 (19). This is another feature that is common between the mutants that block the D-channel at the entrance (D132N and D132A) and the G204D mutant which blocks the channel in the middle.

However, one difference between these mutants is that removing subunit III is by itself sufficient to stimulate the activity of the D132A or D132N mutants (19) whereas the subunit III depletion of the G204D mutant acts to further block the activity of the mutant enzyme. Subunit III has been shown to be required for rapid proton uptake through the D-channel at physiological pH (31). However, it also seems that removing subunit III exposes a cryptic, albeit inefficient, proton entry to the D-channel that is below the level of G204 but above the level of D132. Hence, in the D132N or D132A mutants, there is partial relief of the block caused by the mutant (19). However, with the G204D mutant the effect is like having a double block in the channel, and activity is virtually nil. It has been suggested (19) that a reasonable candidate for the proton entry point exposed by removal of subunit III might be His26 in subunit I. The location of this residue, near D132, would be consistent with the observations in the current work.

In summary, the current work has demonstrated that the G204D mutant has many properties in common with the

D132N and D132A mutants in which proton flux through the D-channel has been blocked. It is concluded that G204D virtually blocks proton flux through the D-channel by disruption the hydrogen bond network of water molecules necessary for proton diffusion through the channel.

## ACKNOWLEDGMENT

We thank Dr. Jonathan Hosler for suggestions and information on subunit III depletion assay.

## REFERENCES

1. Aagaard, A., and Brzezinski, P. (2001) Zinc Ions Inhibit Oxidation of Cytochrome *c* Oxidase by Oxygen, *FEBS Lett.* 494, 157–160.
2. Ferguson-Miller, S., and Babcock, G. T. (1996) Heme/Copper Terminal Oxidases, *Chem. Rev.* 7, 2889–2907.
3. Wikström, M. (2004) Cytochrome *c* Oxidase: 25 Years of the Elusive Proton Pump, *Biochim. Biophys. Acta* 1655, 241–247.
4. Michel, H. (1998) The Mechanism of Proton Pumping by Cytochrome *c* Oxidase, *Proc. Natl. Acad. Sci. U.S.A.* 95, 12819–12824.
5. Michel, H. (1999) Cytochrome *c* Oxidase: Catalytic Cycle and Mechanisms of Proton Pumping—A Discussion, *Biochemistry* 38, 15129–15140.
6. Iwata, S., Ostermeier, C., Ludwig, B., and Michel, H. (1995) Structure at 2.8 Å Resolution of Cytochrome *c* Oxidase from *Paracoccus denitrificans*, *Nature* 376, 660–669.
7. Fetter, J. R., Qian, J., Shapleigh, J., Thomas, J. W., Garcia-Horsman, A., Schmidt, E., Hosler, J., Babcock, G. T., Gennis, R. B., and Ferguson-Miller, S. (1995) Possible Proton Relay Pathways in Cytochrome *c* Oxidase, *Proc. Natl. Acad. Sci. U.S.A.* 92, 1604–1608.
8. Garcia-Horsman, J. A., Puustinen, A., Gennis, R. B., and Wikström, M. (1995) Proton Transfer in Cytochrome *bo3* Ubiquinol Oxidase of *Escherichia coli*: Second Site Mutations in Subunit I that Restore Proton Pumping in the Decoupled Mutant Asp135Asn, *Biochemistry* 34, 4428–4433.
9. Brädén, M., Tomson, F. L., Gennis, R. B., and Brzezinski, P. (2002) Identification of the Entry Point of the K-proton-Transfer Pathway in Cytochrome *c* Oxidase, *Biochemistry* 41, 10794–10798.
10. Wikström, M., Jasaitis, A., Backgren, C., Puustinen, A., and Verkhovsky, M. I. (2000) The Role of the D- and K-pathways of Proton Transfer in the Function of the Haem-copper Oxidases, *Biochim. Biophys. Acta* 1459, 514–520.
11. Rulten, M., Kannt, A., Bamberg, E., Fendler, K., and Michel, H. (2002) Reduction of Cytochrome *c* Oxidase by a Second Electron Leads to Proton Translocation, *Nature* 417, 99–102.
12. Konstantinov, A. A., Siletsky, S., Mitchell, D., Kaulen, A., and Gennis, R. B. (1997) The Roles of the Two Proton Input Channels in Cytochrome *c* Oxidase from *Rhodobacter sphaeroides* Probed by the Effects of Site-Directed Mutations on Time-Resolved Electrogenic Intraprotein Proton Transfer, *Proc. Natl. Acad. Sci. U.S.A.* 94, 9085–9090.
13. Fetter, J., Sharpe, M., Qian, J., Mills, D., Ferguson-Miller, S., and Nicholls, P. (1996) Fatty Acids Stimulate Activity and Restore Respiratory Control in a Proton Channel Mutant of Cytochrome *c* Oxidase, *FEBS Lett.* 393, 155–160.
14. Ädelroth, P., Svensson-Ek, M., Mitchell, D. M., Gennis, R. B., and Brzezinski, P. (1997) Glutamate 286 in Cytochrome *aa3* from *Rhodobacter sphaeroides* is Involved in Proton Uptake During the Reaction of the Fully reduced Enzyme with Dioxygen, *Biochemistry* 36, 13824–13829.
15. Pawate, A. S., Morgan, J., Namslauer, A., Mills, D. A., Brzezinski, P., Ferguson-Miller, S., and Gennis, R. B. (2002) A Mutation in Subunit I of Cytochrome Oxidase from *Rhodobacter sphaeroides* Results in an Increase in Steady-State Activity but Completely Eliminates Proton Pumping, *Biochemistry* 41, 13417.
16. Pfützner, U., Hoffmeier, K., Harrenga, A., Kannt, A., Michel, H., Bamberg, E., Richter, O.-M. H., and Ludwig, B. (2000) Tracing the D-Pathway in Reconstituted Site-Directed Mutants of Cytochrome *c* Oxidase from *Paracoccus denitrificans*, *Biochemistry* 39, 6756–6762.
17. Brzezinski, P., and Larsson, G. (2003) Redox-driven Proton Pumping by Heme-copper Oxidases, *Biochim. Biophys. Acta* 1605, 1–13.
18. Namslauer, A., Pawate, A., Gennis, R. B., and Brzezinski, P. (2003) Redox-Coupled Proton Translocation in Biological Systems: Proton Shuttling in Cytochrome *c* Oxidase, *Proc. Natl. Acad. Sci. U.S.A.* 100, 15543–15547.
19. Mills, D. A., Tan, Z., Ferguson-Miller, S., and Hosler, J. P. (2003) A Role for Subunit III in Proton Uptake into the D Pathway and a Possible Proton Exit Pathway in *Rhodobacter sphaeroides* Cytochrome *c* Oxidase, *Biochemistry* 42, 7410–7417.
20. Mitchell, D. M., and Gennis, R. B. (1995) Rapid Purification of Wildtype and Mutant Cytochrome *c* Oxidase from *Rhodobacter sphaeroides* by Ni<sup>2+</sup>-NTA Affinity Chromatography, *FEBS Lett.* 368, 148–150.
21. Hiser, C., Mills, D. A., Schall, M., and Ferguson-Miller, S. (2001) C-Terminal Truncation and Histidine-tagging of Cytochrome *c* Oxidase Subunit II Reveals the Native Processing Site, Shows Involvement of the C-terminus in Cytochrome *c* Binding, and Improves the Assay for Proton Pumping, *Biochemistry* 40, 1606–1615.
22. Jasaitis, A., Verkhovsky, M. I., Morgan, J. E., Verkhovskaya, M. L., and Wikström, M. (1999) Assignment and Charge Translocation Stoichiometries of the Major Electrogenic Phases in the Reaction of Cytochrome *c* Oxidase with Dioxygen, *Biochemistry* 38, 2697–2706.
23. Rigaud, J.-L., Mosser, G., Lacapere, J.-J., Olofsson, A., Levy, D., and Ranck, J.-L. (1997) Bio-Beads: An Efficient Strategy for Two-Dimensional Crystallization of Membrane Proteins, *J. Struct. Biol.* 118, 226–235.
24. Verkhovsky, M. I., Morgan, J. E., and Wikström, M. (1995) Control of Electron Delivery to the Oxygen Reduction Site of Cytochrome *c* Oxidase: A Role for Protons, *Biochemistry* 34, 7483–7491.
25. Tomson, F. L., Morgan, J. E., Gu, G., Barquera, B., Vygodina, T. V., and Gennis, R. B. (2003) Substitutions for glutamate 101 in subunit II of cytochrome *c* oxidase from *Rhodobacter sphaeroides* result in blocking the proton-conducting K-channel, *Biochemistry* 42, 1711–1717.
26. Morgan, J. E., Verkhovsky, M. I., Puustinen, A., and Wikström, M. (1995) Identification of a “Peroxy” Intermediate in Cytochrome *bo3* of *Escherichia coli*, *Biochemistry* 34, 15633–15637.
27. Mills, D. A., and Hosler, J. P. (2005) Slow Proton Transfer Through the Pathways for Pumped Protons in Cytochrome *c* Oxidase Induces Suicide Inactivation of the Enzyme, *Biochemistry* 44, 4656–4666.
28. Hosler, J. P. (2004) The Influence of Subunit III of Cytochrome *c* Oxidase on the D Pathway, the Proton Exit pathway and Mechanism-based Inactivation in Subunit I, *Biochim. Biophys. Acta* 1655, 332–339.
29. Svensson-Ek, M., Abramson, J., Larsson, G., Tornroth, S., Brzezinski, P., and Iwata, S. (2002) The X-ray Crystal Structures of Wild-type and EQ(I-286) Mutant Cytochrome *c* Oxidases from *Rhodobacter sphaeroides*, *J. Mol. Biol.* 321, 329–339.
30. Smirnova, I. A., Ädelroth, P., Gennis, R. B., and Brzezinski, P. (1999) Aspartate-132 in Cytochrome *c* Oxidase from *Rhodobacter sphaeroides* is Involved in a Two-step Proton Transfer during Oxo-Ferryl Formation, *Biochemistry* 38, 6826–6833.
31. Gilderson, G., Salomonsson, L., Aagaard, A., Gray, J., Brzezinski, P., and Hosler, J. (2003) Subunit III of Cytochrome *c* Oxidase of *Rhodobacter sphaeroides* is Required to Maintain Rapid Proton Uptake through the D Pathway at Physiologic pH, *Biochemistry* 42, 7400–7409.
32. Humphrey, W., Dalke, A., and Schulten, K. (1996) VMD: Visual Molecular Dynamics, *J. Mol. Graphics* 14, 33–38.

BI051141M